Manipulating the metal-to-insulator transition of $NdNiO_3$ films by orbital polarization

J. J. Peng,[1] C. Song,[1,*] M. Wang,[2] F. Li,[1] B. Cui,[1] G. Y. Wang,[1] P. Yu,[2] and F. Pan[1,†]

[1]*Key Laboratory of Advanced Materials (MOE), School of Materials Science and Engineering, Tsinghua University, Beijing 100084, China*

[2]*Department of Physics, Tsinghua University, Beijing 100084, China*

(Received 8 March 2016; revised manuscript received 6 May 2016; published 1 June 2016)

We investigate the film thickness dependent metal-to-insulator transition temperature (T_{MIT}) of $NdNiO_3$ films under tensile and compressive strain states. For the films exceeding the critical thickness for strain relaxation, T_{MIT} varies gradually with the film thickness caused by strain relaxation. The variation tendency differs dramatically for the films below the critical thickness: an increase (decrease) of T_{MIT} with increasing the film thickness for the case of tensile (compressive) strain, which is attributed to the decaying of orbital polarization. As the overlap of O $2p_{x,y}$ orbits with Ni $3dx^2-y^2$ orbits determines T_{MIT}, a decrease of x^2-y^2 orbital occupation with increasing film thickness would reduce the orbital overlap and resultant enhanced T_{MIT} for tensile strained films, while their compressive counterparts do the opposite. Our findings identify the importance of orbital polarization in regulating the metal-to-insulator transitions, opening up a new perspective for orbital physics in transition metal oxides.

DOI: 10.1103/PhysRevB.93.235102

I. INTRODUCTION

The metal-to-insulator transitions (MIT) in complex oxides are often precursors to exotic ground states, such as high temperature superconductivity, colossal magnetoresistance, and different types of charge-, spin-, and orbital-ordered states [1–3]. The charge-transfer nickelate family $RENiO_3$ (RE = rare earth elements) with dramatic MIT has been one of the most fascinating systems for designing innovative oxide interface and heterostructures in the past decade. Understanding and controlling MIT in this specific family is not only interesting from the fundamental physics point of view but also provides great opportunities for future electronic devices, ultimately establishing general design rules for engineering desired phases in complex oxide heterostructures [4–9].

Interpretations of the MIT phenomenon in $NdNiO_3$ center upon whether the transition falls under a Mott-Hubbard or charge-transfer paradigm. Strain engineering for MIT is proved to be effective in controlling MIT of $NdNiO_3$ because the MIT behavior under compressive strain is found to be completely quenched in vast contrast to that of bulk $NdNiO_3$ [10]. Meanwhile, strain engineering is achieved through the strain-induced simultaneous modulation of chemical bond length and bond angle, due to the complexity and sensitivity of which some obscure results frequently occur, i.e., the MIT can still be observed in the case of compressive strain [5,11]. Those contradictory observations point out that strain driven modification of the chemical bond length and bond angle is inadequate to give a satisfying answer to the complicated MIT system.

Another important factor that has to be taken into account is orbital polarization, i.e., orbital-lattice interactions alter the crystal field symmetry and remove the cubic twofold e_g electron degeneracy by favoring either x^2-y^2 or $3z-r^2$ orbits [12]. Previous publications demonstrated that the electron transfer MIT mechanism is associated with the occupation of the Ni orbits and their greater hybridization with the O $2p$ orbits [13,14]. Note that the most serious restriction prohibiting the nickelates from replicating high T_c cuprate superconductors lies in the difficulty in fully removing the orbital degeneracy of the nickelates, hinting the importance of orbital occupation in the transport properties of nickelates [15–18]. Thus, it is highly expected that the orbital polarization would have a dramatic effect on the MIT, although it has not yet be demonstrated; thus, this orbital polarization concept can be considered as a routine to rationalize MIT of many complex oxide systems especially for nickel systems [8,13,14].

In this paper, we demonstrate that the variation of MIT transition temperature (T_{MIT}) with increasing $NdNiO_3$ film thickness (t) originates from the decaying of orbital polarization for the films below the critical thickness (t_c), while strain relaxation is responsible for the variation of T_{MIT} for the films exceeding the critical thickness. As we build the linkage between orbital polarization and MIT, the remarkable capacity of orbital occupation to modulate MIT of this strongly correlated systems are demonstrated.

II. EXPERIMENT

$NdNiO_3$ films were grown on $SrTiO_3$ (STO) and $LaAlO_3$ (LAO) (100) substrates by pulse laser deposition (PLD) from a stoichiometric $NdNiO_3$ target. A series of samples were then prepared at a temperature of 770 °C under an oxygen pressure of 100 mTorr. The layer-by-layer growth mode is identified by reflection high-energy electron diffraction (RHEED), which enables precise calculation of film thickness at atomic level. After growth, the samples were then cooled down to room temperature under an oxygen pressure of 300 Torr at a rate of 10 K/min to reduce some of the oxygen vacancies. Ni L-edge x-ray absorption spectroscopy (XAS) measurements were carried out in total electron yield (TEY) mode at room temperature at Beamline BL08U1A of Shanghai Synchrotron Radiation Facility (SSRF). The background vacuum level was 8×10^{-7} Torr. The spectra normalization was made through dividing the spectra by a factor so that the L_3 pre-edge and L_2 postedge have identical intensities for the two polarizations. After that, the spectra were normalized to the maximum of L_3

*songcheng@mail.tsinghua.edu.cn

†panf@mail.tsinghua.edu.cn

 ©2016 American Physical Society

edge [9,19,20]. The x-ray diffraction (XRD) was conducted at an operating voltage and filament current of 40 kV and 200 mA, respectively. Reciprocal space mapping (RSM) of (103) plane was conducted by high resolution XRD to quantify the strain state of the films. In-plane transport property is measured with the van der Pauw method in a Quantum Design Physical Property Measurement System (PPMS) at temperatures ranging from 20 to 300 K in a cooling process.

III. RESULTS AND DISCUSSION

Figure 1 shows the temperature dependent resistance (*R*-*T*) curves for $NdNiO_3$ films with film thickness ranging from 5 to 200 unit cells (u.c.) on STO and LAO substrates, which exert tensile and compressive strain on the films, respectively. As shown in the figure, films on both STO and LAO substrates possess MIT, in vast contrast to the quench of MIT transitions observed for some compressive strained nickelate films [4,6]. The room temperature resistance of $NdNiO_3$ films on the LAO substrate are lower than those on the STO substrate, inconsistent with previous reports [6,11]. The most eminent feature of Figs. 1(a) and 1(b) is that the transition temperature T_{MIT} varies strongly with film thickness t. Note that T_{MIT} is determined as the temperature, where dR/dT changes its sign, e.g., the temperature with the resistivity minimum. The T_{MIT} of each curve is marked by an open circle in the figure. For the films on the tensile STO substrate, the 20 u.c. thick film shows MIT at a temperature of 152 K. Further increasing t, T_{MIT} first increases to a peak value of 215 K for the 45 u.c. film and then shows a small margin of decrease until an almost saturated state of T_{MIT} of about 200 K is achieved. The films on the compressive LAO substrate display an entirely different characteristic. As displayed in Fig. 1(b), the 5 u.c. film displays a sharp MIT with a T_{MIT} about 154 K. Increasing t reduces T_{MIT} persistently until a lowest value of 85 K is obtained for the 60 u.c. film. After that, T_{MIT} changes gradually and then saturates at a lower value of almost 115 K compared with those on the STO substrate. In addition, note that films on STO substrates with t less than 15 u.c. show an insulting behavior without MIT, whereas the films on LAO substrates as thin as 5 u.c. display a sharp MIT, which will be discussed below.

A summary of t dependent T_{MIT} is depicted in Fig. 1(c). As depicted in the figure, T_{MIT} first increases with t and then decreases for films on STO substrates, while the films on the LAO substrates have a distinct trend. Nevertheless, a turning point around 45 and 60 u.c. indicated by the vertical dashed lines, where strain relaxation usually initiates, is present for the films on STO and LAO substrates, respectively. It is then deduced that the decrease (increase) of T_{MIT} after the dashed lines on the STO (LAO) substrate could be attributed to strain relaxation because both of them have the trend to approach bulk behavior. It is also expected that apparent strain relaxation occurs at a critical thickness (t_c) of 45 u.c. and 60 u.c. for films on the STO and LAO substrate, respectively.

To confirm the strain effect, we performed XRD of film, with t being 10, 20, 25, 30, 45, 60, 75, 100, and 200 u.c. for both substrates, as depicted in Fig. 2. As shown in the figure, the clear (004) peaks of $NdNiO_3$ films are appended on the right (left) side of the STO (LAO) peak, indicative of tensile (compressive) strain exerted on $NdNiO_3$ films. More impor-

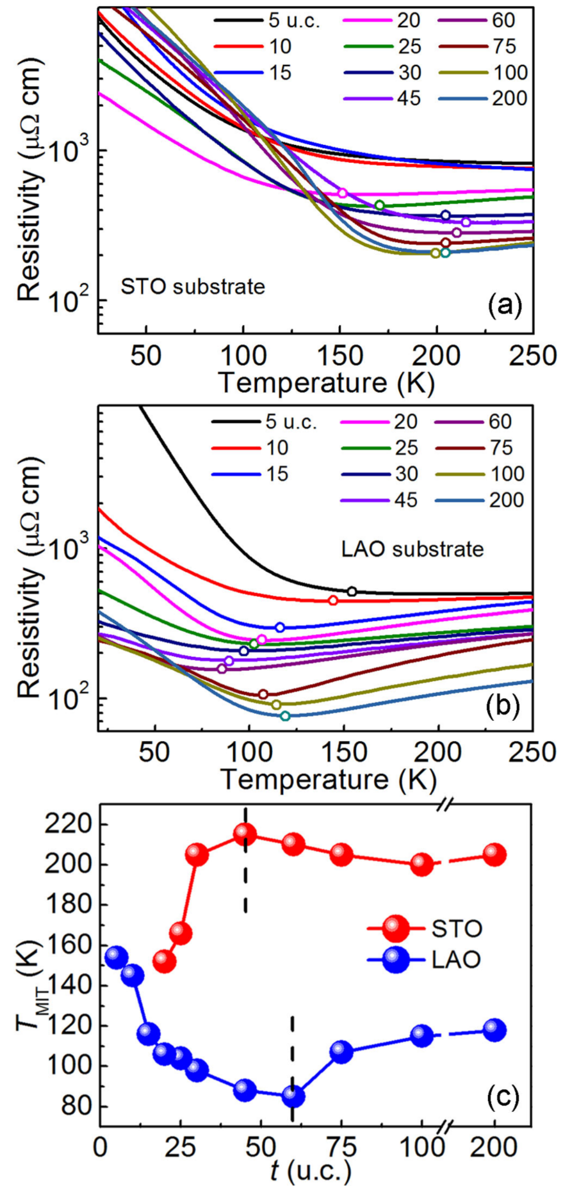

FIG. 1. *R*-*T* curves for a variety of $NdNiO_3$ films with different thicknesses (t) grown on (a) STO substrate and (b) LAO substrate. Only the range from 20 to 250 K is shown, although it is measured from 20 to 300 K .The transition temperature (T_{MIT}) of each curve is indicated by an open circle. (c) A summary of T_{MIT} for films with different thicknesses. The red and blue balls label those on STO and LAO substrates, respectively. The lines are only a guide for the eyes.

tantly, for the films on the STO substrate, the peak positions of $NdNiO_3$ films with t less than 45 u.c. are unchanged, indicating that there is no obvious strain relaxation for the films in this range. However, a gradual but apparent peak shift to a lower angle is detected for films thicker than 45 u.c. Different from the films on the STO substrate, the peak positions remain almost unmoved for 25, 45, and 60 u.c. films on the LAO substrates until an obvious shift occurs for the 75 u.c. film. It is, thus, inferred that there is no detectable strain relaxation for films below 45 and 60 u.c. for films on STO and LAO substrates, respectively; namely, the critical thickness t_c is 45 and 60 u.c. for films under tensile and compressive strain. The critical thickness on LAO

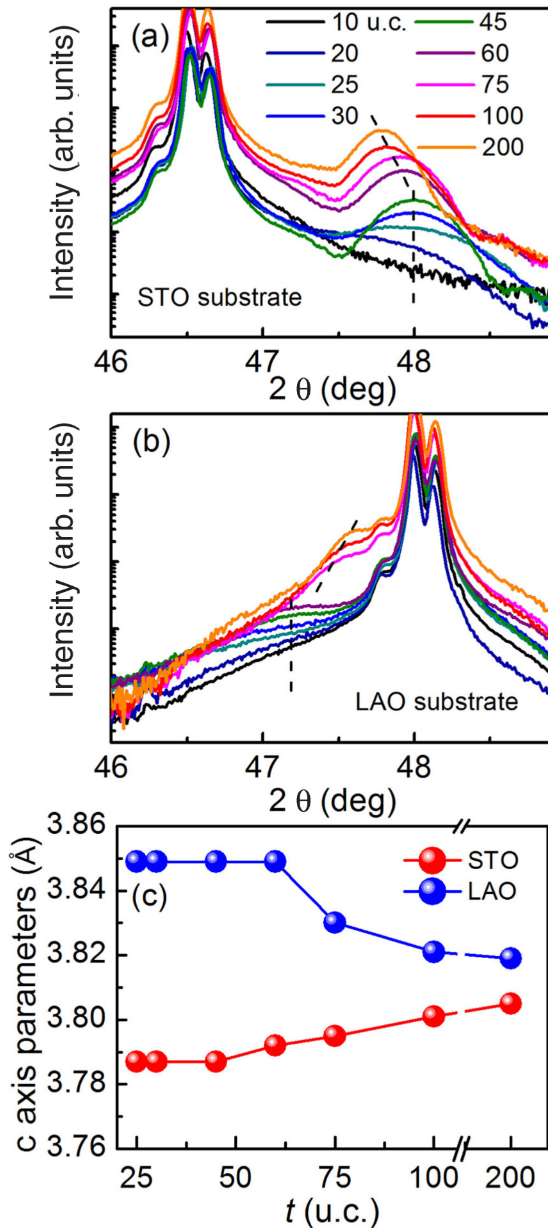

FIG. 2. The XRD spectra of $NdNiO_3$, with t being 10, 20, 25, 30, 45, 60, 75, 100, and 200 u.c. on (a) STO substrate and (b) LAO substrate. The dashed lines denote the position of the peaks. The spectra are shifted vertically for easy recognition. (c) A summary of c axis lattice parameters of films with different thicknesses on both substrates.

substrate is larger than that of STO substrates, most likely due to that $NdNiO_3$ films are under less compressive strain, in accordance with our previous expectation.

To be more specific, we calculated the c axis (out-of-plane) lattice constants according to the XRD spectra, as depicted in Fig. 2(c). As it is clearly shown in the figure, the out-of-plane lattice constant of the films below t_c on STO substrate is 3.787 Å, much smaller than 3.849 Å of those on LAO substrate due to the tensile (compressive) strain caused contraction (expansion) along the out-of-plane direction. For the films above t_c, strain relaxation prompts a recovery of out-of-plane

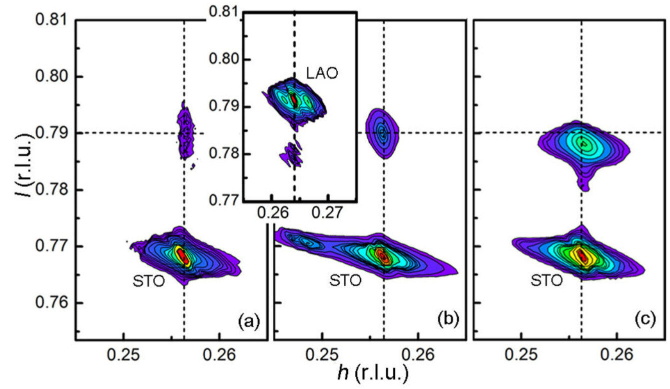

FIG. 3. The RSM of (103) plane of (a) 25 u.c., (b) 45 u.c., and (c) 75 u.c. $NdNiO_3$ film on a STO substrate. The RSM of 45 u.c. film on a LAO substrate is shown in the inset. r.l.u. = reciprocal lattice units.

lattice constants to approach a bulk value of 3.803 Å for both strain states, although there is still some difference between the films on STO and LAO substrates.

One further aspect to be examined is the in-plane structure. We have conducted RSM of (103) plane of the films on STO and LAO substrates, as shown in Fig. 3. The RSM is a powerful method to quantify the strain state, which can be identified by the intensity distribution in the vicinity of the detected Bragg peak. Peaks with identical h (l) values correspond to crystalline material with identical in-plane (out-of-plane) lattice constants. Figures 3(a) and 3(b) show that the peaks of the 25 and 45 u.c. films on the STO substrate have identical h values with the substrate, signaling epitaxial growth, while the 75 u.c. film displays a shift to a larger value, reflecting a reduction of in-plane lattice constant caused by strain relaxation. Concerning the l values of those films, the peaks' positions of 25 and 45 u.c. films are almost the same, while that of the 75 u.c. film is much lower, indicating an increase of the out-of-plane lattice constant caused by strain relaxation. The RSM of 45 u.c. film, as shown in the inset, has identical h values with that of LAO substrates, confirming the epitaxial growth, while the relaxation for films above t_c can be confirmed by the XRD peak shift in Fig. 2(b). Thus, both out-of-plane and in-plane lattice constants have assured epitaxial growth below t_c and strain relaxation above t_c.

Recalling the t dependent T_{MIT} in Fig. 1(c), it is clear that strain relaxation caused change of lattice constant is playing a role for films above t_c (45 u.c. for STO and 60 u.c. for LAO). In other words, the strain relaxation causes lattice constants to approach bulk value and resultantly increases (decreases) the T_{MIT} of films under compressive (tensile) strain with the trend to approach bulk $NdNiO_3$ behavior. Now, it can be safely concluded that strain relaxation is responsible for the variation of T_{MIT} above t_c. For films below t_c, the variation of T_{MIT} as a function of film thickness remains a question of interest to be explored.

To investigate the origin of the variation of T_{MIT} below t_c, we then proceed to performed x-ray linear dichroism (XLD) to exam the orbital occupation of those films. The x-ray absorption profiles were measured with σ polarization and π polarization of the incident light at an incident angle of 30°,

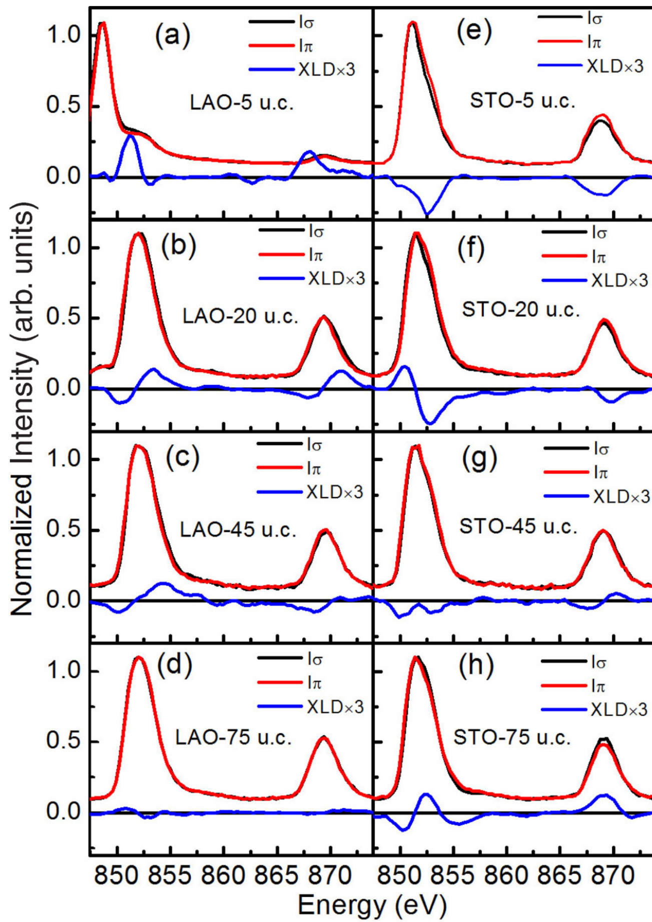

FIG. 4. The XAS spectra measured with linearly polarized light for $NdNiO_3$ films, with t being 5, 20, 45, and 75 u.c. on (a)–(d) the LAO substrate and (e)–(h) the STO substrate. The normalized difference spectra $[I_\sigma(E) - I_\pi(E)]$ are shown directly below the corresponding spectra.

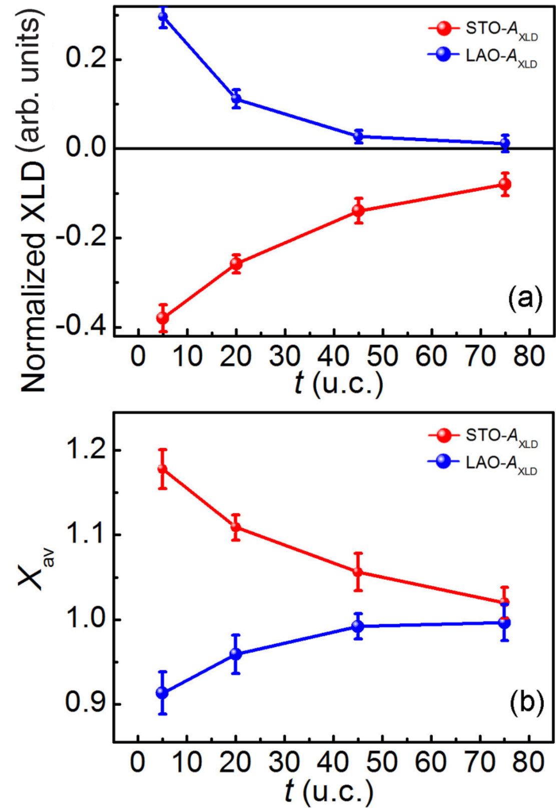

FIG. 5. (a) The $A_{\rm XLD}$ and (b) calculated spatially averaged hole ratio $X_{\rm av}$ obtained via the sum rule (1) by Eq. (1). The XLD measurements were carried out a couple of times for the error bar.

as described in the literature [20]. To analyze the Ni L-edge XLD in a qualitative way, the difference between the XAS in-plane ($E/\!/\sigma$) and out-of-plane ($E/\!/\pi$) components, namely, $I_\sigma - I_\pi$, is employed to elucidate Ni $3d$ orbital occupation. The area under XLD around the L_3 and L_2 peaks ($A_{\rm XLD}$; 847.5–874 eV) represents the difference between the relative occupancies of the $3z-r^2$ [2] and x^2-y^2 orbits [20]. In qualitative analysis, positive $A_{\rm XLD}$ is observed in the spectra of films grown on compressive LAO substrates (in the left panel of Fig. 4), signalling preferred $3z-r^2$ [2] orbital occupation, while negative $A_{\rm XLD}$ exists in the spectra of films grown on tensile STO substrates (in the right panel of Fig. 4), suggesting preferred x^2-y^2 orbital occupation. In addition, note that both positive and negative $A_{\rm XLD}$ are decaying as we increase t, reflecting the decaying of preferred orbital occupation. For the 75 u.c. films on both substrates, an almost orbital degenerate state is observed. We, then, conclude that the films exhibit t dependent orbital occupation on both STO and LAO substrates.

To obtain an accurate quantitative estimation, the sum rule is applied for the observed linear dichroism. Although for σ polarization, the measured intensity is directly related to $E/\!/x$, the intensity for $E/\!/z$ is deduced from $I_z = 4/3I_\pi - 1/3I_\sigma$ [17]. The sum rule relates the ratio of holes in the Ni e_g orbits to the energy-integrated XAS intensities across the Ni L edge $I_{x,z} = \int_{L_{2,3}} I_{x,z}(E)dE$ for in-plane (x) and out-of-plane (z) polarization [16]

$$X_{\rm av} = \frac{h_{3z^2-r^2}}{h_{x^2-y^2}} = \frac{3I_z}{4I_x - I_z}, \quad (1)$$

where $X_{\rm av}$ is the spatially averaged hole ratio, $h_{x^2-y^2}$ and $h_{3z^2-r^2}$ are the hole occupancy numbers of x^2-y^2, and $3z-r^2$ [2] orbits, respectively. A summary of t dependent $A_{\rm XLD}$ and $X_{\rm av}$ is given in Figs. 5(a) and 5(b), respectively. For the films on the LAO substrate, positive $A_{\rm XLD}$ is descending to almost zero with increasing t, demonstrating the descending occupation of the preferred orbital $3z-r^2$ [2] orbits. Similarly negative $A_{\rm XLD}$ is ascending to almost zero with increasing t for those on STO substrates, demonstrating the decaying occupation of the preferred orbital x^2-y^2 orbits. It is easy to understand that there is a nearly orbital degenerate state for strain relaxed 75 u.c. films, just like orbital degenerate bulk $NdNiO_3$ [6].

Tracing back to t dependent $T_{\rm MIT}$ in Fig. 1(c), strain relaxation caused change of lattice constant accounts for the change of $T_{\rm MIT}$ on the tail. Recalling the XRD results, no variation of XRD peak can be detected for the films below the critical thickness, indicating that neither exact change of crystal structure nor detectable change of lattice constant is responsible for the variation of $T_{\rm MIT}$. Thus, it is deduced that for those films below t_c, the variation of $T_{\rm MIT}$ should be related to the decaying orbital polarization. Previous reports

demonstrated an increase in the overlap of the O $p_{x,y}$, and Ni x^2-y^2 orbits would greatly reduce the resistance and enhance the metallic nature of nickel oxides [21]. On the other hand, the interpretation of the MIT in the charge-transfer mechanism emphasizes the band gap opening between the transition metal d states and the oxygen $2p$ orbits. On the basis of these two arguments, the occupation of Ni orbits is pivotal in determining the gap opening process and then manipulates the transition temperature. That is to say, an enhancement of x^2-y^2 orbital occupation would boost in-plane overlap of Ni and O orbits and reduce T_{MIT}. Thus, a reasonable interpretation of t dependent T_{MIT} can be drawn. For those on STO substrates, an increase of t would be accompanied by a reduction of x^2-y^2 orbital occupation then promote the T_{MIT} to higher temperatures. On the other hand, for those on LAO substrates, an increase of t would be accompanied by a reduction of $3z-r^2$ [2] orbital occupation, or in a relative point of view, an enhancement of x^2-y^2 orbital occupation then reduces T_{MIT} to a lower temperature. Note that the overlap of O $p_{x,y}$ and Ni x^2-y^2 orbits is pivotal in determining the T_{MIT} but not in the way that it directly influences the resistivity. The resistivity is determined by the overall overlap of O orbits with Ni orbits, not just the Ni x^2-y^2 orbits [22]. The different Ni-O bond bending and stretching modes result in different ground states for tensile and compressive strained films. The larger overlap of O and Ni orbits decreases the resistivity of compressive strained films. Note that the prevailing of oxygen vacancies further increases the resistivity of tensile strained films by reducing the hole carriers of NNO. A combination of these two factors promote a more metallic state for compressive strained films and a resultant lower transition temperature compared with its tensile counterpart, just as we observed in Fig. 1(c). Up to now, a reasonable interpretation of the variation of T_{MIT} with t can be drawn, based on the change of orbital polarization, although it remains to be explored what is the origin of the change of orbital polarization.

An alternative to investigate the origin of the change of orbital polarization is to compare the XAS spectra with different film thicknesses and check whether any detectable change of valence states with film thickness is present. Taking into account that soft x-ray has a shallow probing depth around 6 nm, the XAS mainly reflects the surface valence states of the film. Figures 6(a) and 6(b) display the XAS of films grown on STO and LAO substrates, respectively. The XAS at Ni L edge is sensitive to Ni $2p_{3/2,1/2} \rightarrow 3d$ dipole transitions, providing information on the unoccupied Ni $3d$ state and related Ni valence states. Separated by the spin-orbit splitting of the Ni $2p$ core hole, the spectra exhibit two broad multiplets generally defined as Ni L_3 and L_2 peak, respectively. Considering the shallow probing depth of x-ray, it is unavoidable that the additional La M_4 from LAO substrates superimposes on the XAS of films with t less than 10 u.c. on LAO substrates.

As indicated in Fig. 6(a), there is a gradual shift of L_3 peak towards higher energy direction (from 851.15 to 851.86 eV) when increasing the film thickness t from 5 u.c. to 200 u.c. on STO substrates. However, no such shift is detected for the films on LAO substrates with all the L_3 peaks locating at 852 eV, as shown in Fig. 6(b). As reported, tensile strain would enhance the formation of oxygen vacancies evidenced by theoretical calculations that tensile strain lowers the formation

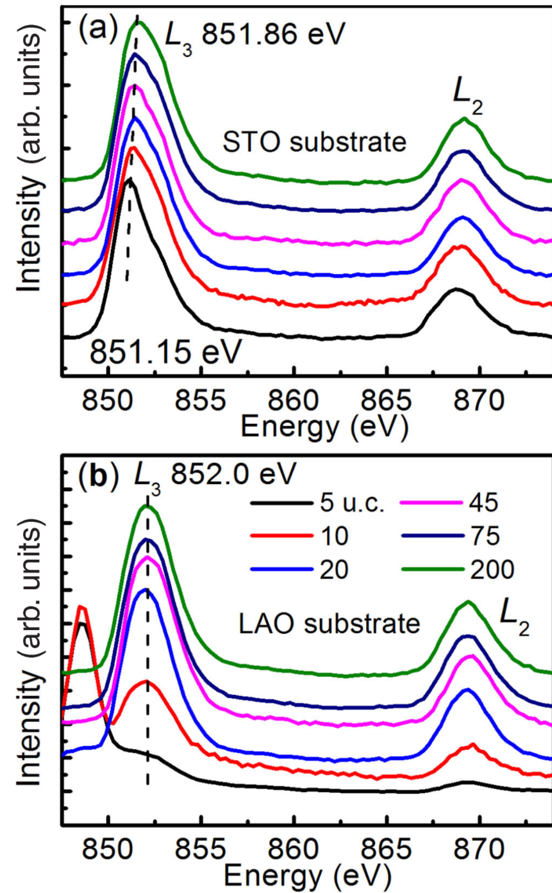

FIG. 6. Normalized XAS of $NdNiO_3$ films with different thicknesses on (a) the STO substrate and (b) the LAO substrate, with t being 5, 10, 20, 45, 75, and 200 u.c. The dashed lines denote the position of the peaks. The spectra are shifted vertically for easy recognition.

energy of oxygen vacancies [23]. Thus, an energy difference of about 0.85 eV reflects the abundance of oxygen vacancies in ultrathin $NdNiO_3$ films on STO substrates compared with those on LAO substrates. The insulating nature of the films less than 20 u.c. on STO substrates is also closely related to the abundance of oxygen vacancies in the whole film [24]. Also, the gradual shift of the L_3 peak towards lower energy direction with t decreasing for those films on STO substrates reflects that more oxygen vacancies exist in thinner films [25]. The absence of such a phenomenon on LAO substrates may indicate the infertility of oxygen vacancies, let alone talking about the variation of oxygen vacancies for different thickness. Furthermore, the thickest (200 u.c.) films can be regarded as fully relaxed, and the minor energy difference between those on two substrates indicates strain from substrates has a negligible effect in determining surface electronic structure.

When film is grown coherently on a substrate with a different lattice constant, one way to accommodate the epitaxial strain is through structural distortions, such as changing the internal bond lengths or changing the angle or pattern of rotations and tilts of the oxygen octahedra [26]. In addition to this, another possible method to accommodate coherent epitaxial growth is a change in the defect profile. The volume increase associated with biaxial tensile strain is likely to

increase the concentration of oxygen vacancies, while in the opposite direction compressive strain should increase the concentration of cation vacancies due to the concomitant charge balancing oxidation of cations with smaller ionic radii at higher oxidation states [22]. In our tensile strained films, a large amount of oxygen vacancies are presented, with an uneven distribution in the defect profile that gives rise to the observed Ni valence state and related decaying of orbital polarization. For the compressive strain films, cation vacancies prevail, an uneven distribution of which is incapable to influence the Ni valence state but can be reflected by the decaying of orbital polarization. We attribute the decaying of orbital polarization with t to be related to the defect depth profile, and the decaying of orbital polarization accounts for the variation of T_{MIT} for films below the critical thickness. For films above the critical thickness, apparent strain relaxation causes the change of lattice constants that induces the change of T_{MIT}.

IV. CONCLUSION

We observe a variation of T_{MIT} with film thickness for films under tensile and compressive strain. For films below critical thickness, the variation of T_{MIT} originates from the decaying of orbital polarization with the increase of film thickness. The reason is that the overlap of O $2p_{x,y}$ orbits with Ni $3dx^2-y^2$ orbits determines the band gap opening and accordingly determines T_{MIT}. Thus, a decrease of x^2-y^2 orbital occupation with increasing film thickness would greatly increase T_{MIT} for those under tensile strain, while for those under compressive strain, a reduction of $3z-r^2$ [2] orbital occupation, or in a relative point of view, an enhancement of x^2-y^2 orbital occupation with film thickness is responsible for the decrease of T_{MIT}. For films above critical thickness, strain relaxation is playing a role in the gradual shift of T_{MIT}. Our paper illustrates the remarkable capacity of orbital occupation to modulate MIT of these strongly correlated systems, opening up a new perspective to tailor and benefit from orbital physics in transition metal oxides.

ACKNOWLEDGMENTS

The authors acknowledge Beamline BL08U1A in the Shanghai Synchrotron Radiation Facility for x-ray absorption spectroscopy and x-ray linear dichroism measurements. This paper was supported by the National Natural Science Foundation of China (Grants No. 51322101 and No. 51571128) and National Hi-Tech (R&D) Project of China (Grant No. 2014AA032904).

[1] R. S. Dhaka, T. Das, N. C. Plumb, Z. Ristic, W. Kong, C. E. Matt, N. Xu, K. Dolui, E. Razzoli, M. Medarde, L. Patthey, M. Shi, M. Radović, and J. Mesot, Phys. Rev. B **92**, 035127 (2015).
[2] G. Chen, C. Song, C. Chen, S. Gao, F. Zeng, and F. Pan, Adv. Mater. **24**, 3515 (2012).
[3] A. M. H. R. Hakimi, M. G. Blamire, S. M. Heald, Marzook S. Alshammari, M. S. Alqahtani, D. S. Score, H. J. Blythe, A. M. Fox, and G. A. Gehring, Phys. Rev. B **84**, 085201 (2011).
[4] D. Meyers, S. Middey, M. Kareev, M. van Veenendaal, E. J. Moon, B. A. Gray, J. Liu, J. W. Freeland, and J. Chakhalian, Phys. Rev. B **88**, 075116 (2013).
[5] R. Scherwitzl, P. Zubko, I. G. Lezama, S. Ono, A. F. Morpurgo, G. Catalan, and J. M. Triscone, Adv. Mater. **22**, 5517 (2010).
[6] J. Liu, M. Kargarian, M. Kareev, B. Gray, P. J. Ryan, A. Cruz, N. Tahir, Y.-D. Chuang, J. Guo, J. M. Rondinelli, J. W. Freeland, G. A. Fiete, and J. Chakhalian, Nat. Commun. **4**, 2714 (2013).
[7] K. Kurita, A. Chikamatsu, K. Shigematsu, T. Katayama, H. Kumigashira, T. Fukumura, and T. Hasegawa, Phys. Rev. B **92**, 115153 (2015).
[8] A. David, Y. F. Tian, P. Yang, X. Y. Gao, W. N Lin, A. B. Shah, J. M Zuo, W. Prellier, and T. Wu, Sci. Rep. **5**, 10255 (2015).
[9] J. J. Peng, C. Song, B. Cui, F. Li, H. J. Mao, G. Y. Wang, and F. Pan, Appl. Phys. Lett. **107**, 182904 (2015).
[10] J. Liu, M. Kareev, B. Gray, J. Kim, P. Ryan, B. Dabrowski, J. Freeland, and J. Chakhalian, Appl. Phys. Lett. **96**, 233110 (2010).
[11] L. Wang, S. Ju, L. You, Y. Qi, Y.-W. Guo, P. Ren, Y. Zhou, and J. L. Wang, Sci. Rep. **5**, 18707 (2015).
[12] D. Pesquera, G. Herranz, A. Barla, E. Pellegrin, F. Bondino, E. Magnano, F. Sánchez, and J. Fontcuberta, Nat. Commun. **3**, 1189 (2012).
[13] M. H. Upton, Y. Choi, H. Park, J. Liu, D. Meyers, J. Chakhalian, S. Middey, J.-W. Kim, and P. J. Ryan, Phys. Rev. Lett. **115**, 036401 (2015).
[14] J. W. Freeland, J. Liu, M. Kareev, B. Gray, J. W. Kim, P. Ryan, R. Pentcheva, and J. Chakhalian, Europhys. Lett. **96**, 57004 (2011).
[15] X. Wang, H. T. Dang, and A. J. Millis, Phys. Rev. B **84**, 014530 (2011).
[16] M. Wu, E. Benckiser, M. W. Haverkort, A. Frano, Y. Lu, U. Nwankwo, S. Brück, P. Audehm, E. Goering, S. Macke, V. Hinkov, P. Wochner, G. Christiani, S. Heinze, G. Logvenov, H.-U. Habermeier, and B. Keimer, Phys. Rev. B **88**, 125124 (2013).
[17] A. S. Disa, D. P. Kumah, A. Malashevich, H. Chen, D. A. Arena, E. D. Specht, S. Ismail-Beigi, F. J. Walker, and C. H. Ahn, Phys. Rev. Lett. **114**, 026801 (2015).
[18] J. Chaloupka and G. Khaliullin, Phys. Rev. Lett. **100**, 016404 (2008).
[19] D. Yi, J. Liu, S. Okamoto, S. Jagannatha, Y. C. Chen, P. Yu, Y. H. Chu, E. Arenholz, and R. Ramesh, Phys. Rev. Lett. **111**, 127601 (2013).
[20] J. J. Peng, C. Song, B. Cui, F. Li, H. J. Mao, Y. Y. Wang, G. Y. Wang, and F. Pan, Phys. Rev. B **89**, 165129 (2014).
[21] D. P. Kumah, A. S. Disa, J. H. Ngai, H. H. Chen, A. Malashevich, J. W. Reiner, S. Ismail-Beigi, F. J. Walker, and C. H. Ahn, Adv. Mater. **26**, 1935 (2014).
[22] M. K. Stewart, J. Liu, M. Kareev, J. Chakhalian, and D. N. Basov, Phys. Rev. Lett. **107**, 176401 (2011).
[23] U. Aschauer, R. Pfenninger, S. M. Selbach, T. Grande, and N. A. Spaldin, Phys. Rev. B **88**, 054111 (2013).
[24] A. Tiwari and K. P. Rajeev, Solid State Commun. **109**, 119 (1999).
[25] B. Cui, C. Song, H. J. Mao, H. Q. Wu, F. Li, J. J. Peng, G. Y. Wang, F. Zeng, and F. Pan, Adv. Mater. **27**, 6651 (2015).
[26] J. M. Rondinelli and N. A. Spaldin, Adv. Mater. **23**, 3363 (2011).